

Thermal Analysis of Poly(vinyl fluoride)

MARK D. HANES¹ and JEROME B. LANDO^{2,*}

¹Phillips Petroleum, Research & Development, Building 71C, Bartlesville, Oklahoma 74004; ²Department of Macromolecular Science, Case Western Reserve University, Cleveland, Ohio 44106

SYNOPSIS

A sub- T_m transition at approximately 50°C in poly(vinyl fluoride) has been attributed to a number of physical factors. We have studied this effect using differential scanning calorimetry. The rate dependence of the endothermic peak at approximately 50°C indicates that it is a second order transition. However, the recovery behavior is time dependent. It is observed in perfect head-to-tail, perfectly linear polymer and thus is not a consequence of head-to-head or tail-to-tail defects or branch points. The transition appears to be a time dependent rearrangement of the polymer chains. © 1993 John Wiley & Sons, Inc.

INTRODUCTION

Semicrystalline poly(vinyl fluoride) (PVF) exhibits several thermal transitions consisting of a melting endotherm and a minimum of four sub- T_m transitions. The melting temperature of PVF has been shown to be very sensitive to the HH/TT content. Cais and Kometani¹ developed a synthetic method that provides control over the HH/TT content and studied a series of samples containing defect contents ranging from 0 to 30%. They showed that the melting point for the samples decreased with increasing HH/TT content and varied from 230°C for a HT sample to 160°C for a sample containing 30% HH/TT units.

The number of sub- T_m transitions, although not unique to PVF,² has led to some confusion over their interpretation.³⁻⁷ Boyer² and, later, Enns and Simha⁸ attributed the four sub- T_m transitions to a sub- T_g local-mode motion occurring in the range -100 to -53°C, a lower T_g occurring between -36 and 10°C, an upper T_g occurring in the range 40–82°C, and a premelting phase transition in the range 110–170°C. The exact values for the transitions are dependent on both the method of measurement⁸ and the crystallinity of the sample.² It has also been proposed that regic defects in the sample influence the upper T_g . Boyer suggested that the upper T_g may be due to a slower crystallization rate for HH defects resulting in exclusion from the crystalline regions, thus giving rise to the transition. Sacher,⁹ on the other hand, reported dielectric loss peaks located at

-18 and +22°C that he associated with the HH sequences and the HT sequences, respectively.

In the present work, we looked at the thermal behavior of PVF in the temperature range 0–250°C by differential scanning calorimetry. The melting point was measured for a series of samples and correlated with the polymerization temperature for several series of radically polymerized PVF. Utilizing the results of Cais and Kometani,¹ the polymerization temperature was correlated to the melting temperature to determine if the polymerization temperature affects the HH/TT content in PVF.

Currently, there are conflicting reports in the literature regarding whether the polymerization temperature influences the HH/TT content of radically polymerized PVF. Based on studies of other vinyl polymers¹⁰ including poly(vinylidene fluoride),¹¹ one would expect the HH/TT content in PVF to be dependent on the polymerization temperature. Such a relationship has been reported by Wilson and Santee¹² and Koenig and Mannion.¹³ However, work done by Gorlitz et al.¹¹ found no relation between the two.

We have also investigated the transition occurring at approximately 50°C that has previously been labeled as the upper glass transition. The physical origins for this peak are not completely understood or agreed upon. It is hoped that this work can contribute toward a more complete understanding of the origins of this peak.

EXPERIMENTAL

Differential scanning calorimetry runs were made on a series of PVF samples. The scans were run on

* To whom correspondence should be addressed.

a Perkin-Elmer series 7 DSC instrument. The samples were weighed on an Perkin-Elmer AD-2 auto-balance and crimp sealed in DuPont DSC pans. The base line of the machine was adjusted to remove any slope or curvature and the calibration of the instrument was checked with indium ($T_m = 156.6^\circ\text{C}$) and tin ($T_m = 231.88^\circ\text{C}$). All scans were made with an empty pan placed in the second sample holder and the instrument placed in a nitrogen glove box.

The melting behavior was investigated by the following procedure: The samples were loaded at 25°C and the heat flow was allowed to stabilize. Each sample was then scanned from 25 to 250°C at $20^\circ\text{C}/\text{min}$. They were held at 250°C for 1 min and then cooled to 25°C at a rate of $20^\circ\text{C}/\text{min}$. The samples were held at 25°C until the heat flow stabilized. A second run was made following the procedure of the first run.

The low-temperature transition was studied in the temperature range 0 – 100°C . The sample was loaded at 0°C and the heat flow was allowed to stabilize. All runs were made from 0 to 100°C , held for 1 min, then cooled to 0°C . All scans were made at $20^\circ\text{C}/\text{min}$ unless otherwise stated.

Melting Behavior

Results

Three sets of radically polymerized samples were studied: a set of two commercial samples polymer-

ized at a temperature of 90 and 100°C , respectively, under similar reaction conditions; a series of commercial samples polymerized at a nominal temperature of 100°C under varying conditions; and three samples provided by Dr. R. Uschold of DuPont Central Research that were synthesized in the laboratory at 80 , 91 , and 103°C under controlled conditions not possible in the plant. There was also one sample provided by Dr. Cais of AT&T Bells Labs that was a perfect HT polymer. This sample was not produced by the radical polymerization of vinyl fluoride, but by the reductive dechlorination of poly(1-chloro,1-fluoroethylene). This sample was a perfect HT polymer, since in the polymerization of 1-chloro-1-fluoroethylene, for steric and electrostatic reasons, only head-to-tail additions occur. The structure of the Bell Labs sample has been verified by NMR.¹

Figure 1 shows a representative example of a DSC heating scan. Three transitions can be seen in the scan: The first occurs at approximately 50°C and is classified, following the work of Boyer, as the upper T_g . The second transition has been attributed to a premelting transition and produces the change in slope at approximately 130°C . The final transition is the melting endotherm at 200°C .

Figure 2 shows a cooling scan. Only a recrystallization peak is observed at approximately 160°C . Figure 3 shows a second scan of the sample. The low-temperature peak is no longer observed and the

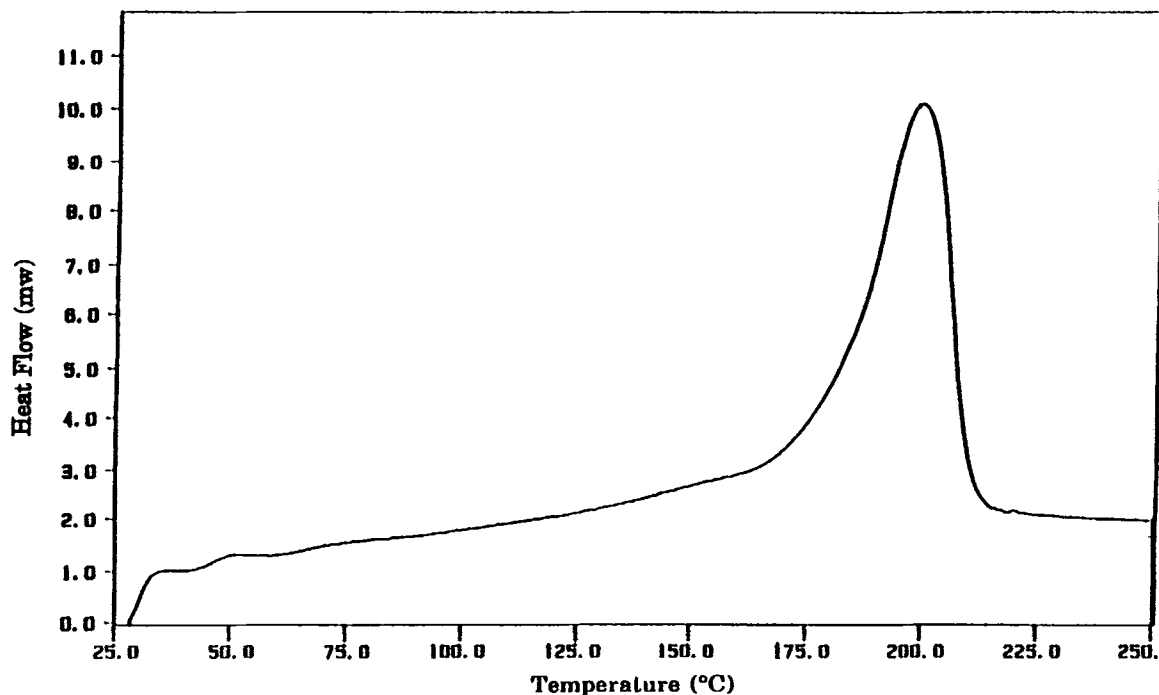


Figure 1 DSC heating scan of as received sample ($20^\circ\text{C}/\text{min}$).

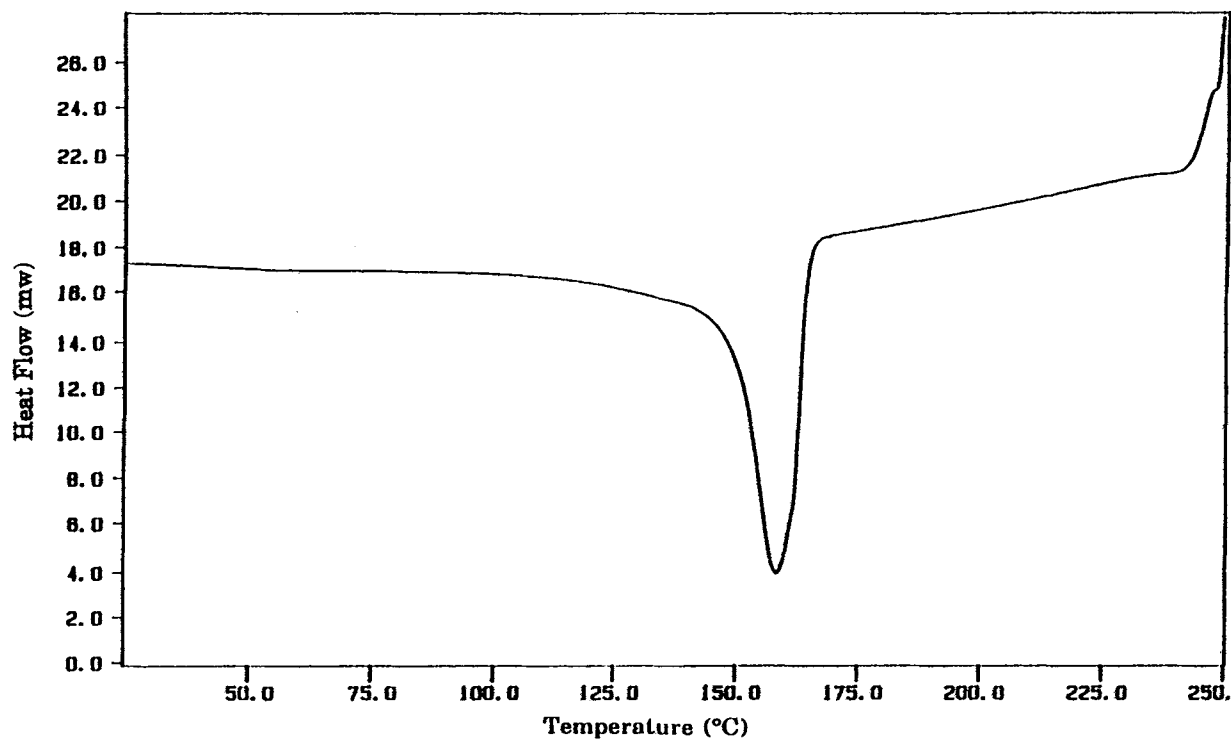


Figure 2 DSC cooling scan of sample (20°C/min).

melting endotherm is sufficiently broad to obscure the premelting transition if, indeed, it is still present.

The melting temperature was measured for all samples and the results are compiled in Table I. The

heat of fusion was not measured for the samples due to difficulty in distinguishing the start of the melting endotherm from the premelting transition. Although it is fairly easy to distinguish the two in Figure 1,

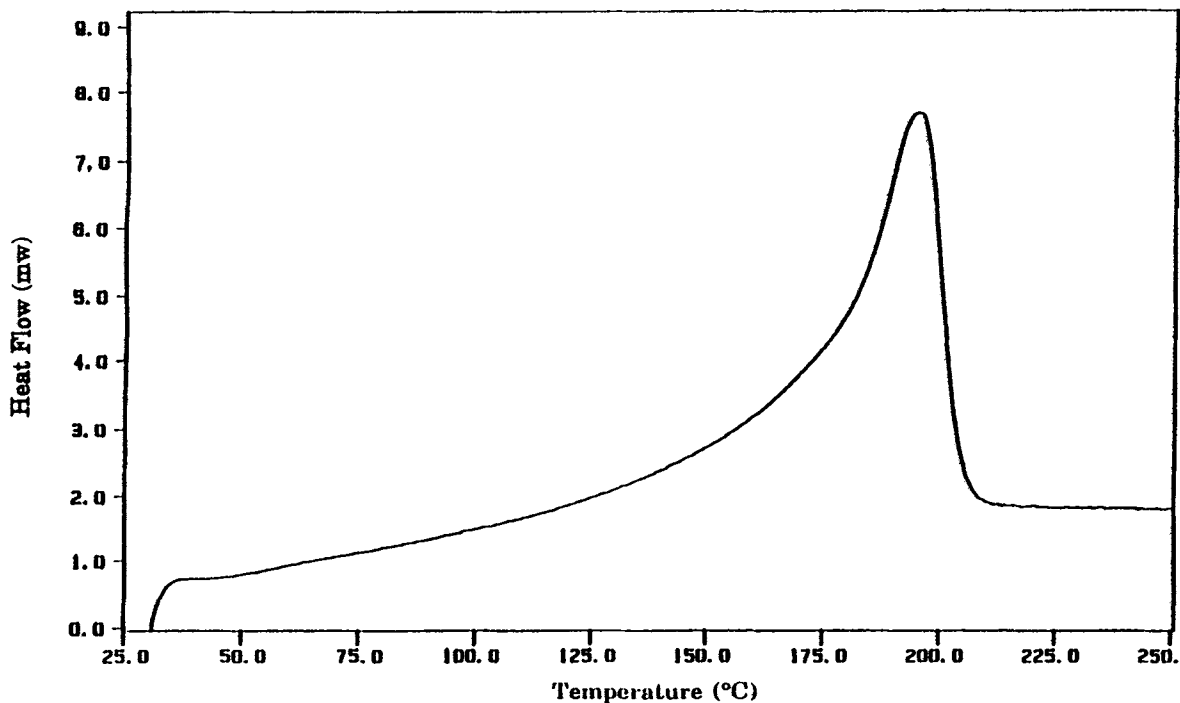


Figure 3 Second DSC heating scan of sample (20°C/min).

Table I Melting Temperature for a Series of PVF Samples

Sample	Polymerization Temp (°C)	Scan #1 (°C)	Scan #2 (°C)
Laboratory			
127c	80.0	199.1	195.3
77	91.0	195.5	192.4
72	103.0	191.7	190.5
Commercial #1			
68e	90.0	195.8	196.7
64a	90.0	193.8	195.2
64c	90.0	196.8	195.4
65a	90.0	194.4	193.7
65b	90.0	194.0	194.3
19c	100.0	191.3	194.1
24b	100.0	193.6	194.1
51g	100.0	193.3	188.5
54a	100.0	190.7	191.8
Commercial #2			
Lo	100.0	193.6	192.8
Hi	100.0	192.7	190.8
1a	100.0	193.3	192.5
1b	100.0	194.5	193.4
2a	100.0	194.5	193.6
3a	100.0	194.5	192.8
4a	100.0	193.8	193.7
5a	100.0	192.8	192.1
11a	100.0	195.5	194.1
12a	100.0	196.0	195.0
13a	100.0	195.1	194.8
14a	100.0	195.4	193.9
Bell Labs sample	—	232.3	(Degraded)

for many of the samples, there was no distinct slope change, but rather a continuous increase in the slope up to the melting point, i.e., the derivative of the slope never progressed through a maximum to indicate the premelting transition.

The melting temperatures were plotted vs. the polymerization temperature and are shown in Figure 4. The commercial samples made at varying temperatures are indicated with a triangle (\blacktriangle), the second set of commercial samples are marked with a cross (\times), and the laboratory samples are marked with a square (\blacksquare). The melting temperatures used were those from the first run. For the commercial samples, the thermal history is known and is the same for all the samples. For the laboratory samples, the thermal histories are not known. However, little difference is observed in the correlation whether the first- or second-run temperatures are used.

Discussion

The melting temperatures determined by DSC are listed in Table I. All the temperatures fall in the range 188–199°C with the exception of the sample synthesized at AT&T Bell Labs. The melting temperature for this sample was 232°C. Although radically polymerized PVF has been reported to contain up to 25% HH/TT defects,¹¹ the Bell Lab sample is a perfect HT structure. This thus reflects the large impact HH/TT defects can have in PVF.

Comparison of the polymerization temperature with the melting temperature is shown in Figure 4.

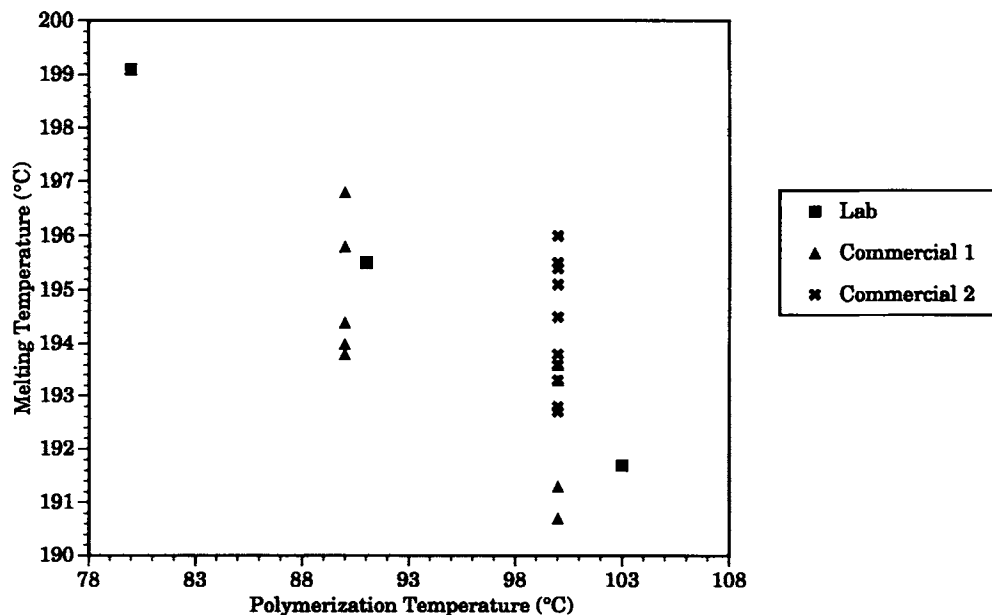


Figure 4 Relationship of the polymerization temperature to the melting temperature.

Overall, it is not clear whether a dependence exists between the melting temperature and the polymerization temperature. However, if the three different classes of samples are examined individually, some trends are observed. When examined by themselves, the first set of commercial samples, which were polymerized at varying temperatures under controlled conditions, show a definite correlation between the melting temperature and the polymerization temperature. As the polymerization temperature is increased, the melting temperature decreases, implying that the HH/TT content increases. The sample polymerized at 80°C had a melting temperature of 199°C, whereas the sample polymerized at 103°C had a melting point of 192°C. This behavior is typical for radically polymerized fluorinated vinyl compounds.

The laboratory samples show a similar trend. These polymers were polymerized under varying conditions with one set polymerized at 100°C and the other at 90°C. Although there is scatter in the data, in general, the samples polymerized at 90°C had a higher melting point than those at 100°C. The samples polymerized at 90°C had an average melting temperature of 195°C and those polymerized at 100°C melted at an average temperature of 192°C.

For the set of commercial samples polymerized at 100°C, there is a range of temperatures at which they melt, from 193 to 196°C. Thus, they appear to cast doubt on the reliability of the melting temperature-polymerization temperature relationship. However, evaluation of these samples is complicated by the polymerization conditions. The polymerization takes place in a reactor with a temperature gradient of 6°C from the entrance to the exit of the reactor. Hence, assuming the melting temperature is dependent on the polymerization temperature, the melting temperatures of our samples would be sensitive to the polymerization conversion ratio and extent of reaction as a function of position within the reactor. If the reaction conditions were such that the majority of the reaction occurred at the entrance of the reactor, the polymer structure would reflect a polymerization temperature of close to 97°C. Conversely, if the majority of the reaction occurred at the exit of the reactor, the apparent polymerization temperature would be close to 103°C. Consequently, the melting temperature values should not all be plotted vs. a polymerization temperature of 100°C, but over the range 97–103°C. This would explain some of the scatter in the data. The factors that could influence this are the residence time in the reactor, the initiator concentration, the initiation and polymerization kinetics, and the reactor design. Unfortunately, not all these variables are known and

so a correlation to the present data is not possible. Thus, this set of samples is not useful in examining the relationship between the melting temperature and polymerization temperature.

Low-temperature Transition

Results

The maxima of the low-temperature transition was measured and the values are listed in Table II. The peak ranged in temperature from 47 to 64°C. The behavior of the peak was studied by three different methods: First, the rate dependence of the peak was investigated. Four samples were heated from 0 to 100°C at rates of 5, 10, 20, and 40°C/min. A noticeable shift to higher temperature and increased peak size was observed as the rate was increased (see Fig. 5).

The second method was an annealing study where

Table II Glass Transition Temperature for a Series of PVF Samples

Sample	Polymerization Temp (°C)	Peak Position (°C)
<u>Laboratory</u>		
127c	80.0	51.0
77	91.0	47.0
72	103.0	48.0
<u>Commercial #1</u>		
68e	90.0	57.0
64a	90.0	54.0
64c	90.0	58.0
65a	90.0	54.0
65b	90.0	54.0
19c	100.0	53.0
24b	100.0	56.0
51g	100.0	55.0
54a	100.0	55.0
<u>Commercial #2</u>		
Lo	100.0	64.0
Hi	100.0	57.0
1a	100.0	62.0
1b	100.0	63.0
2a	100.0	64.0
3a	100.0	63.0
4a	100.0	60.0
5a	100.0	59.0
11a	100.0	55.0
12a	100.0	56.0
13a	100.0	56.0
14a	100.0	56.0
Bell Labs sample	—	63.0

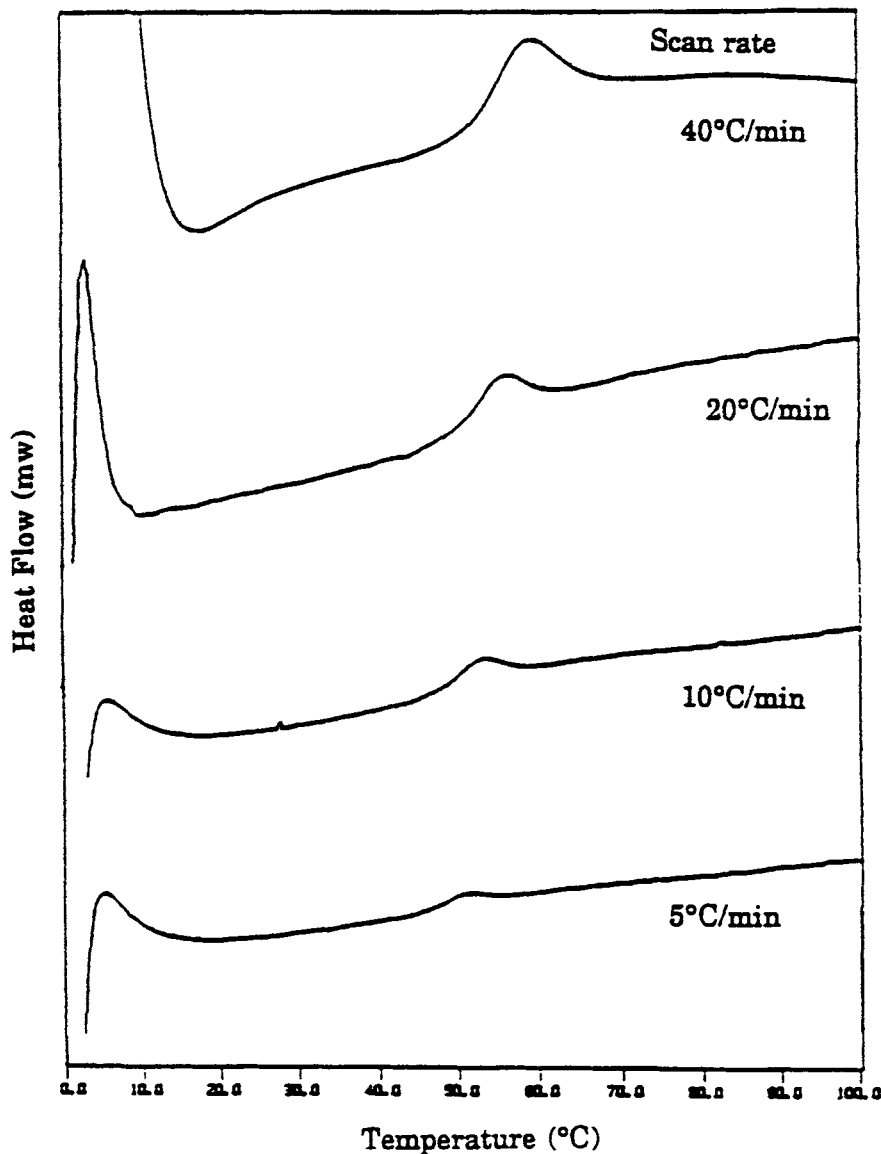


Figure 5 Effect of heating rate on the glass transition.

the sample was heated to 160°C and held for 0, 5, 15, and 30 min. The sample was then cooled and left at room temperature for 8 days. This time period was required for reformation of the peak. The samples were then scanned from 0 to 100°C. No significant change in peak size or position was detected (see Fig. 6).

The last method investigated the recovery behavior of the peak. A sample was run from 0 to 100°C and cooled back to 0°C. The sample was then immediately rerun, rerun after a delay of 1 h, rerun after a delay of 6 h, and rerun after a delay of 8 days. The peak was not observed when immediately re-scanned and was just visible after a delay of 1 h. At 1 h, the peak was shifted to a lower temperature and

was of much lower intensity relative to the initial peak. At longer delay times, the peak recovered and shifted back to its original position and intensity (see Fig. 7).

Discussion

The peak positions are listed in Table II. There appears to be no correlation with any of the polymerization variables. In addition, the values reported for each sample should not be considered characteristic values due to a strong dependence of the peak on the crystallinity.² The values reported are the temperatures measured for each sample in their

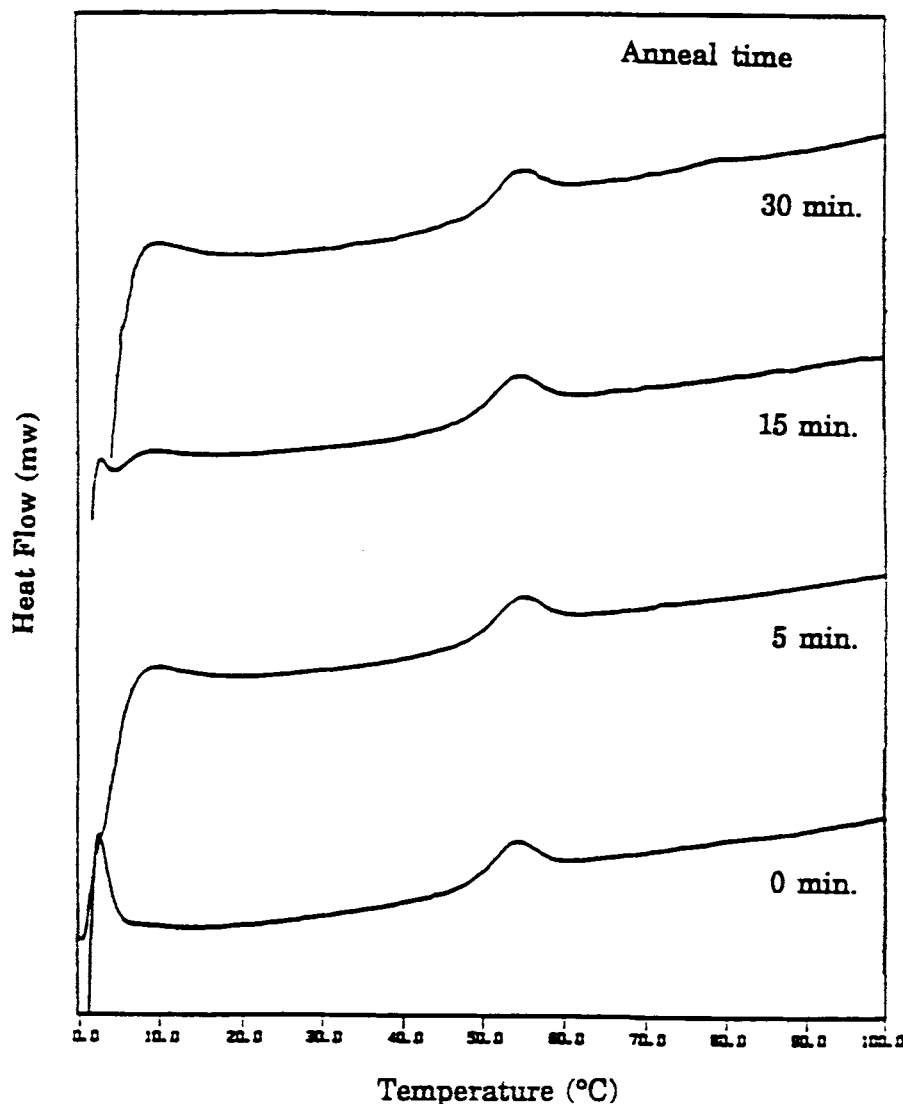


Figure 6 Effect of annealing time on the glass transition ($20^{\circ}\text{C}/\text{min}$).

“as-received” condition. The thermal history of the sample was observed to have a direct bearing on the peak position and intensity.

One interesting result was the observation of the peak for the sample from Bell Labs. Since this sample had no HH/TT defects, the presence of the peak definitely precludes any relationship between the peak and HH/TT defects. As an aside, the reasoning for HH/TT structures producing an upper T_g can also be applied to branched structures. Commercial PVF has been shown by NMR to be a branched structure, but the Bell Labs sample was a linear polymer. Therefore, the observation of the peak for this sample would also indicate that the branched nature of radically polymerized PVF is not responsible for the presence of the transition.

Although the low-temperature transition has been assigned as an upper glass transition,^{2,8} it does

not always exhibit behavior typical of a T_g . The transition is apparent on the first run but is not observed when the sample is immediately rescanned (see Figs. 1 and 3). Considering the fact that the crystallinity is lower in the second run, one would typically expect the intensity of a glass transition to increase. However, Takayanagi¹⁴ proposed that the appearance of an upper T_g is associated with amorphous material that is constrained between crystalline lamellae. The constrained nature of the region results in a lower mobility of the chains and, hence, can produce a second T_g appearing at a higher temperature. This could explain why the transition is not observed immediately after the melting of the sample since the presence of constrained amorphous regions may occur only above a certain level of crystallinity. However, it was observed that melting the sample and then annealing for up to 30 min at 160°C

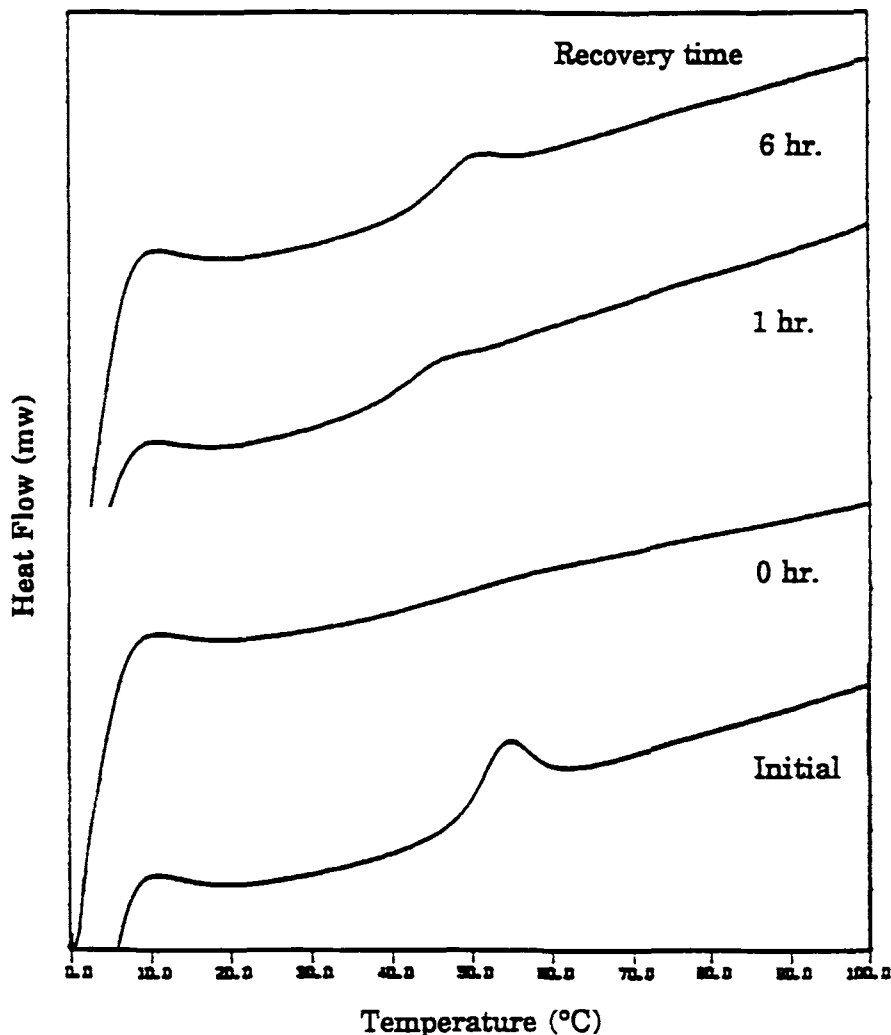


Figure 7 Recovery process of glass transition ($20^{\circ}\text{C}/\text{min}$).

did not cause the peak to reappear. On the other hand, if the sample was melted and left at room temperature for several days, the peak did reappear.

The observation was also made that the loss of the low-temperature peak was not dependent on melting the sample but occurred whenever the sample was heated through the transition. This result raised doubts about the nature and physical origins of the peak. It was also observed that the shape of the peak for some of the samples resembled a first-order transition more than a second order one (see Fig. 8). A second-order transition is associated with a discontinuity in the heat capacity and is evidenced by a step function type transition. This does not describe the scan in Figure 8, which, instead, looks more like a first-order endothermic transition.

Three experiments were performed to clarify the nature of the peak: The first set of scans examined the rate dependence of the peak (see Fig. 5). The

purpose for this experiment was to determine the nature of the transition associated with the peak. The glass transition is known to be rate-dependent, shifting to higher temperatures as the rate is increased. This is the behavior that is observed in Figure 5. In addition, the intensity of the transition also increases, and for this particular sample, the scans at 10 and $20^{\circ}\text{C}/\text{min}$ have a more traditional glass transition shape, albeit with an endothermic cap. What is striking about the dependence is how sensitive the transition is to the rate. The peak is very strong for the rate of $40^{\circ}\text{C}/\text{min}$ and has decreased in intensity by such an extent that at a scan rate of $5^{\circ}\text{C}/\text{min}$ it is almost unobserved. In addition, the scan at $5^{\circ}\text{C}/\text{min}$ has lost the peak shape typical for a T_g . Nonetheless, the rate dependence does confirm that the transition is not endothermic in nature but is associated with a second-order transition.

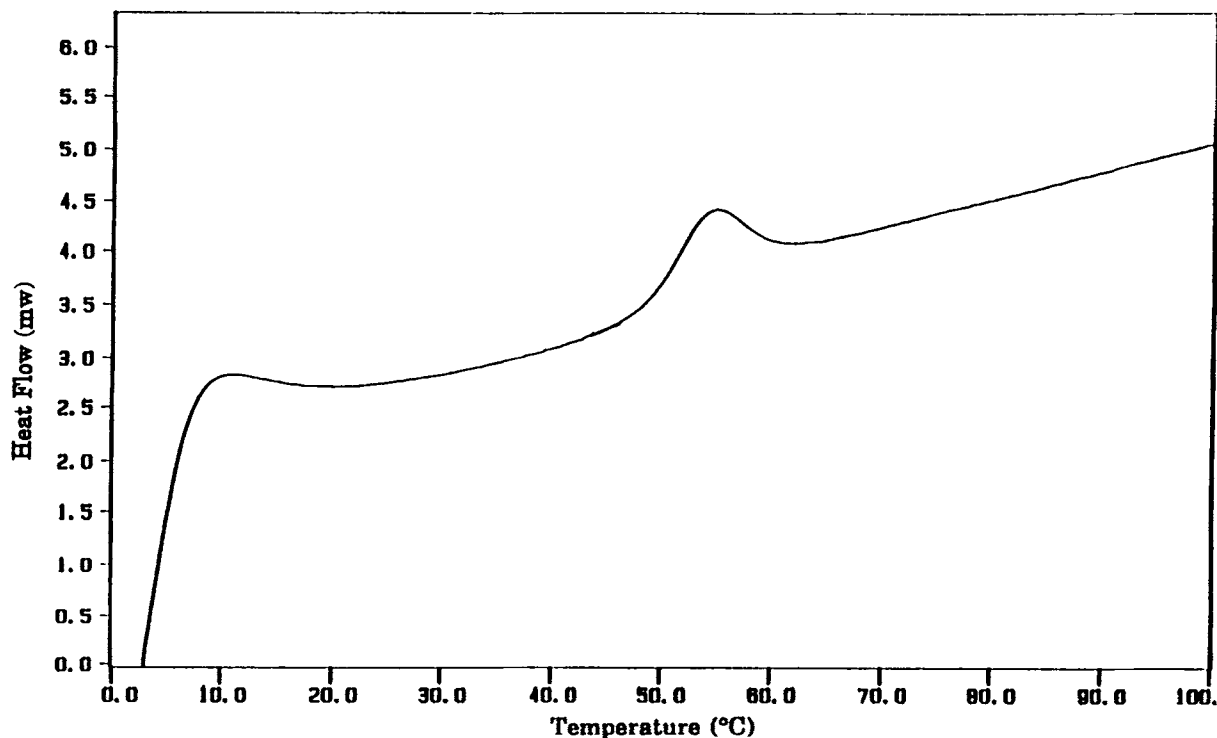


Figure 8 DSC scan of glass transition peak (20°C/min).

The second set of scans examined the effect of annealing (see Fig. 6). The intent here was to alter the crystalline regions by annealing and, consequently, change either the peak position and/or the intensity. If the peak is associated with amorphous regions constrained by crystalline regions, one would expect the peak to disappear if the amorphous material is incorporated into the crystalline regions. On the other hand, if the crystal growth only serves to further constrain the amorphous regions, then the peak would shift to higher temperatures. Observations showed that the annealing had no effect on either the peak position or intensity. However, the annealing process, under these conditions, had only a small effect on the crystallinity and, thus, it is difficult to draw a definite conclusion.

In the last set of scans, the recovery of the peak was monitored (see Fig. 7). The sample was heated to 100°C, cooled to room temperature, and then re-run periodically to monitor the recovery. It was surprising to find the peak disappear without first melting the sample. This could indicate that by heating above the glass transition temperature the amorphous regions are able to relieve constraints by a relaxation process. However, the fact that the peak recovers while the crystalline regions remain unchanged is somewhat confusing. Since the peak does recover, it may have implications about the nature of the constraints.

There are two types of constraints that can be envisioned: a constraint due to pinning the chain on a crystal face and a constraint due to restricted mobility as a result of being confined between two crystal faces. Each case could result in either a stress on the polymer chain or a limitation in the number of possible conformational states of the polymer chain. For a stress on the polymer chain, the chain should be able to simply relax and relieve the constraint. If the chain has restricted conformational mobility, the constraint should be, in a sense, permanent until the sample is melted. Neither of these cases appears to fully explain the recovery behavior observed. Therefore, either the constrained amorphous regions are not the explanation for the peak or, more likely, that the formation of the constraints involves some type of coordinated rearrangement of the chains and thus has some time dependency involved. Rearrangement could be possible since the chains are still above their unconstrained T_g of approximately -20°C .

CONCLUSIONS

In the thermal analysis of PVF, we have observed three transitions, two of which have been investigated. Using the melting temperature as an indication of the HH/TT content, the polymerization

temperature does appear to influence the HH content in PVF. However, from the scatter in the data, it is possible that there are other factors that may also have an influence. In addition, the commercial polymerization has been performed in such a way that one would expect a range in the HH/TT defect content dependent on several variables of the reaction process. However, given the limited temperature range for this study, any conclusions would best be verified by further investigation encompassing a larger range for the polymerization temperature.

The analysis of the glass transition focused on investigating its unusual behavior. The rate dependence of the peak indicates that it is indeed due to a second-order transition. However, the recovery behavior of the peak raises questions as to its physical origins. The fact that it is observed in a perfect HT sample indicates that the transition is not a consequence of either HH/TT defects, as has been suggested, or branch points since neither of these is present in the sample. The fact that PVF experiences a relaxation process, but then reforms with time, may indicate that the transition is associated with a coordinated rearrangement of chains that is time dependent.

The financial support of this work by the Edison Polymer Innovation Corporation and E. I. DuPont DeNemours & Company is gratefully acknowledged.

REFERENCES

1. R. E. Cais and J. M. Kometani, *Polymer*, **29**, 168 (1988).
2. R. F. Boyer, *J. Polym. Sci. Symp.*, **50**, 189 (1975).
3. R. F. Boyer, *J. Polym. Sci. C*, **14**, 3 (1966).
4. A. R. McGhie, G. McGibbon, A. Sharples, and E. J. Stanley, *Polymer*, **13**, 371 (1972).
5. N. Kawasaki and T. Hashimoto, *J. Polym. Sci. A2*, **9**, 2095 (1971).
6. T. Takamatsu and E. Fukada, *Polym. J.*, **1**, 101 (1970).
7. J. B. Enns, M. S. Thesis, Case Western Reserve University, 1975.
8. J. B. Enns and R. Simha, *J. Macromol. Sci. Phys.*, **B13**(1), 11 (1977).
9. E. Sacher, *J. Macromol. Sci.-Phys.*, **B19**(1), 109 (1981).
10. G. Odian, *Principles of Polymerization*, 2 ed., Wiley, New York, 1981, p. 186.
11. M. Gorlitz, R. Minke, W. Trautvetter, and G. Weisgerber, *Angew. Makromol. Chem.*, **29/30**, 137 (1973).
12. C. W. Wilson and E. R. Santee, Jr., *J. Polym. Sci. Part C*, **8**, 97 (1967).
13. J. L. Koenig and J. J. Mannion, *J. Polym. Sci. Part A2*, **4**, 401 (1966).
14. M. Takayanagi, *Pure Appl. Chem.*, **15**, 555 (1967).

Received October 26, 1992

Accepted December 3, 1992